

## Accepted Article

**Title:** Widening the scope of “inherently chiral” electrodes:  
enantiodiscrimination of chiral electroactive probes with planar  
stereogenicity

**Authors:** Sara Grecchi, Serena Arnaboldi, Marcus Korb, Roberto  
Cirilli, Silvia Araneo, Vittoria Guglielmi, Giorgio Tomboni,  
Mirko Magni, Tiziana Benincori, Heinrich Lang, and Patrizia  
Romana Mussini

This manuscript has been accepted after peer review and appears as an Accepted Article online prior to editing, proofing, and formal publication of the final Version of Record (VoR). This work is currently citable by using the Digital Object Identifier (DOI) given below. The VoR will be published online in Early View as soon as possible and may be different to this Accepted Article as a result of editing. Readers should obtain the VoR from the journal website shown below when it is published to ensure accuracy of information. The authors are responsible for the content of this Accepted Article.

**To be cited as:** *ChemElectroChem* 10.1002/celc.202000657

**Link to VoR:** <https://doi.org/10.1002/celc.202000657>

Widening the scope of "inherently chiral" electrodes: enantiodiscrimination of chiral electroactive probes with planar stereogenicity

S. Grecchi,<sup>[a]</sup> S. Arnaboldi,<sup>[a]</sup> M. Korb,<sup>[b]</sup> R. Cirilli,<sup>[c]</sup> S. Araneo,<sup>[a]</sup> V. Guglielmi,<sup>[a]</sup> G. Tomboni,<sup>[a]</sup> M. Magni,<sup>[a]</sup> T. Benincori,<sup>[d]</sup> H. Lang\*,<sup>[e]</sup> and P.R. Mussini\*<sup>[a]</sup>

- [a] S. Grecchi, Dr. S. Arnaboldi, Dr. S. Araneo, Dr. V. Guglielmi, G. Tomboni, Dr. M. Magni, Prof. P. R. Mussini  
Dipartimento di Chimica  
Università degli Studi di Milano  
Via Golgi 19, 20133, Milan, Italy  
E-mail: patrizia.mussini@unimi.it
- [b] Dr. M. Korb  
The University of Western Australia, Faculty of Sciences, School of Molecular Sciences,  
35 Stirling Highway, Crawley, Perth, Western Australia 6009, Australia (current address)
- [c] Dr. R. Cirilli  
Centro Nazionale per il Controllo e la Valutazione dei Farmaci  
Istituto Superiore di Sanità  
Viale Regina Elena 299, 00161 Roma, Italy
- [d] Prof. T. Benincori  
Dipartimento di Scienza e Alta Tecnologia  
Università degli Studi dell'Insubria  
Via Valleggio 11, 22100 Como, Italy
- [e] Prof. H. Lang  
Technische Universität Chemnitz, Faculty of Natural Sciences  
Institute of Chemistry, Inorganic Chemistry  
Straße der Nationen 62, 09111 D-09107 Chemnitz, Germany

Supporting information for this article is given via a link at the end of the document. ~~((Please delete this text if not appropriate))~~

**Abstract:** A series of planar-stereogenicity ferrocenes, important as chiral promoters in enantioselective catalysis, is here characterized in terms of relationships between structure and electronic properties. The enantiomers of six selected model cases are then successfully discriminated in voltammetry experiments on electrodes modified with electrodeposited inherently chiral oligomer films, in terms of significant potential differences, specular inverting probe or selector configuration. Small substituent changes do not alter the enantiomer peak sequence, but result in significant modulation of peak potential differences, looking consistent with the availability of chiral/selector matching elements. The present stereogenic plane case, combined with former ones involving stereogenic centres, axes and/or helices, shows that the inherent chirality strategy in electroanalysis can be effective with all four rigid stereogenic elements.

## Introduction

The discrimination and quantification of the enantiomers of chiral probes is of great importance in many applicative fields. Therein, chiral chromatography techniques are commonly applied, particularly for routine determinations<sup>[1]</sup>. However, the electrochemical approach to direct enantiomer discrimination is increasingly emerging as very interesting, and more and more effective strategies and selectors are being considered.<sup>[2-44]</sup> Particularly attractive are voltammetric measurements based on electron transfers at suitable enantiopure chiral interphases resulting in different potentials for the enantiomers of chiral probes<sup>[2,3,21-44]</sup>. The relation between current and concentration could also allow for the determination of the enantiomer concentration, and even, in favourable cases, the estimation of the enantiomeric excess

directly in solution. In this frame, chirality can be implemented at the interphase either by electrode surface modification with a high variety of selectors<sup>[2-5]</sup>, or by choosing a chiral medium or medium component, such as the solvent, the supporting electrolyte, or more effectively, a chiral ionic liquid or even an ionic liquid with chiral additives.<sup>[2]</sup> In particular, outstanding discrimination ability, in terms of large peak potential differences between chiral probe enantiomers, has been recently observed when "inherently chiral" selectors were adopted for the above task. In such selectors both chirality and main functional properties originate from the same element, coinciding in all so far considered examples with the main molecular backbone, which features a tailored torsion with a very high racemization barrier.<sup>[35-44]</sup> A thoroughly investigated model example is provided by the 2,2'-[2-(5,2-bithienyl)]-3,3'-thianaphthene (BT<sub>2</sub>T<sub>4</sub>) electroactive monomer, inherently chiral on account of its *atropisomeric* bibenzothiothiophene core (*i.e.*, with sterically hindered rotation between its two halves). By electrooxidation it enables fast, reproducible electrode modification with films constituted by a mixture of open and cyclic inherently chiral electroactive oligomers (Figure 1)<sup>[35,45]</sup>, resulting in effective enantiodiscrimination of chiral electroactive probes of different nature<sup>[35-38]</sup>. Remarkably, the same inherent chirality strategy has proved successful with other inherently chiral electrodeposited films, either based on different *atropisomeric cores*, *i.e.* bithiophene<sup>[39]</sup> and biindole<sup>[40]</sup>, or on a *helical element* as tetrathia[7]helicene<sup>[41]</sup> (carbohelicene films<sup>[46]</sup> could be also tested). It even held when implemented in ionic liquid media or related additives, again either on account of *atropisomeric elements*, *i.e.* bipyridinium<sup>[42]</sup> or bibenzimidazolium<sup>[43]</sup> salts, or of a helical tetrathiahelicene element<sup>[44]</sup>.

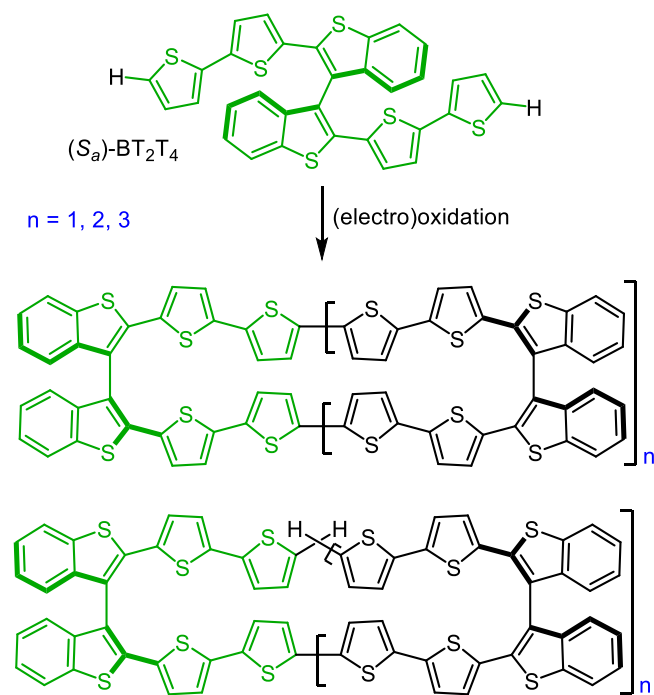


**Figure 1.** The inherently chiral BT<sub>2</sub>T<sub>4</sub> starting monomer in (S<sub>a</sub>) configuration (top) together with general formulas of its cyclic (middle) and open oligomers (bottom) constituting the electrodeposited chiral electrode surface. [35,45]

Thus the inherent chirality strategy has been shown to be of general character, a given selector (be it electrode surface or medium) being able to discriminate the enantiomers of redox probes with different chemical and electrochemical properties [35-44].

However, in such works only three out of the four kinds of rigid stereogenic elements (see key concepts and definitions at SI.1) have been considered in the chiral probes and/or chiral selectors, namely stereocentres (A), stereogenic axes (B), and helices (D, Figure 2).

Still missing is the fourth case, *i.e.* planar stereogenicity (C), including for example paracyclophanes [47-49], ansa compounds [50], chiral tetrathiafulvalenes [51], pillar[n]arenes [52] and metallocenes with at least two different substituents on one of the aromatic rings [53-55]. Actually, the above four stereogenic elements can be fascinatingly related through a common *fil rouge* rationale, starting from the stereocentre, as shown in Figure 2.

A convenient model case for an electrochemistry investigation of planar stereogenicity probes is represented by ferrocenes having at least one cyclopentadienyl ring bearing two different substituents (Table 1, Figure S1) [53].

In fact, the ferrocene group undergoes chemically and electrochemically reversible electron transfer at mild potentials, hardly affected by the solvent (actually, the ferrocene couple is the IUPAC recommended intersolvental reference standard for electrode potentials [56]), but very regularly modulable by the substituent nature and number, which can be rationalized in terms of Hammett's constants [57].

#### A: stereogenic center

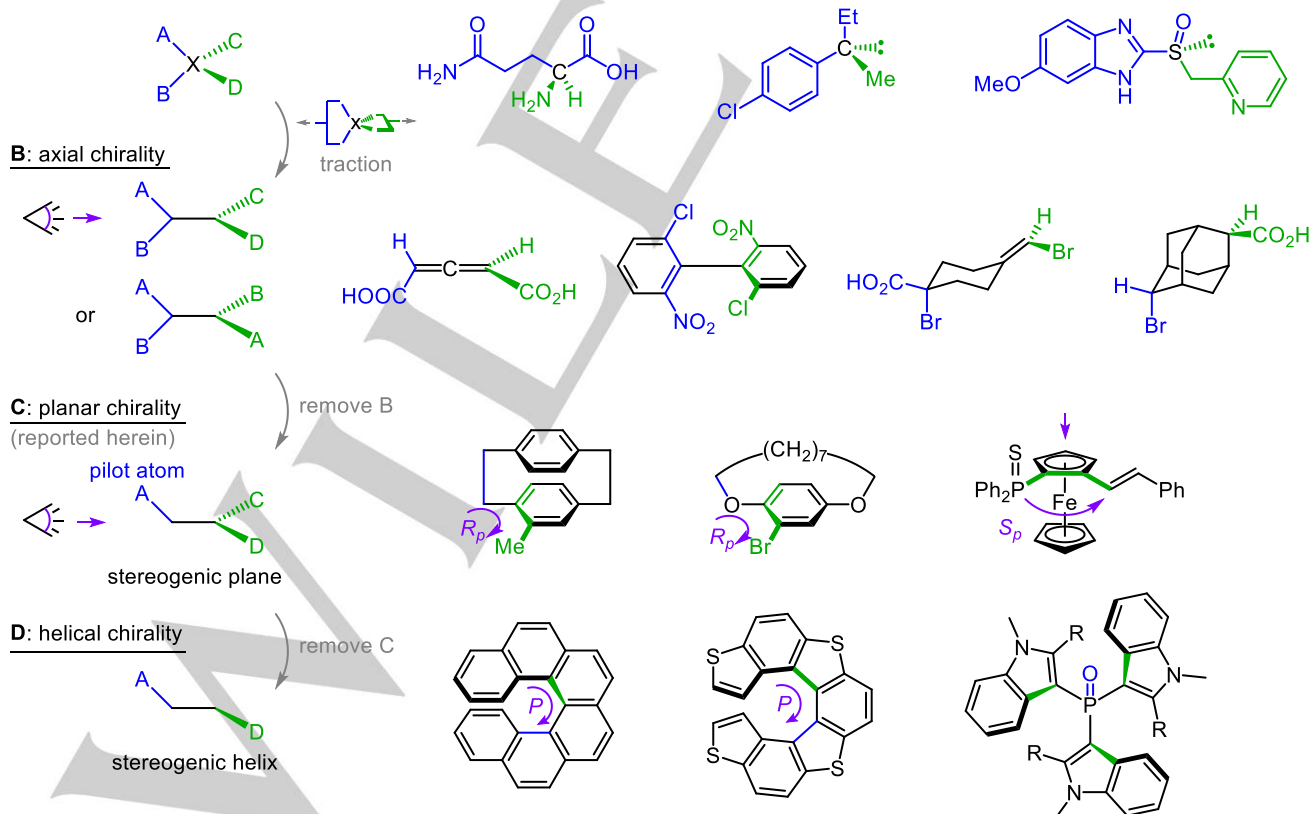


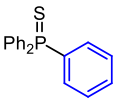
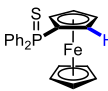
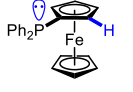
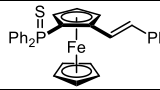
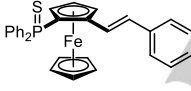
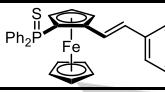
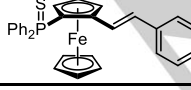
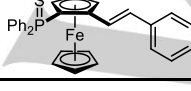
**Figure 2.** The four stereogenic elements, highlighting their logical sequence, and with several examples: (a) central stereogenicity; (b) axial stereogenicity; (c) planar stereogenicity; (d) helical stereogenicity.

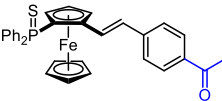
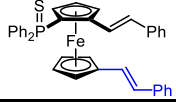
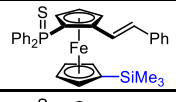
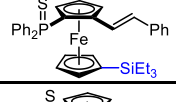
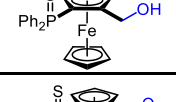
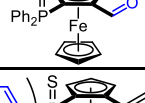
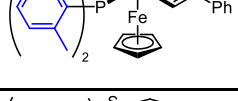
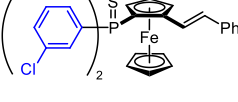
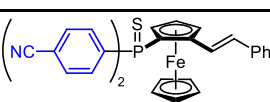
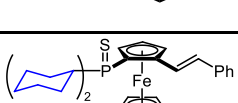
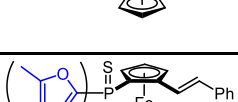
Moreover, ferrocene is important for many fundamental and applicative purposes. For example, it is a very popular redox active label for electroanalysis of non-electroactive probes, particularly in the biological field [58]. Chiral receptors which included ferrocenes with planar stereogenicity have been recently tested by an electrochemical approach with proline-based probes [59]. Ferrocene is also an attractive building block for molecular materials with advanced electrochemical and/or chiroptical properties, e.g. conjugated with heterocyclic systems [60], even chiral [61], in molecular wires [62], and in systems with reciprocally interacting multiple redox centres [63]. Furthermore, it is a suitable candidate for magnetic circular dichroism [64] and, symmetrically, magneto-electrochemistry experiments [65], on account of the ferricinium/ferrocene  $\text{Fc}^+/\text{Fc}$  redox couple including a paramagnetic species. Finally, chiral ferrocenes, including planar stereogenicity ones, gained great applicative interest in the field of asymmetric catalysis, [66-78] on account of attractive features including for example the great stability of the ferrocene group in air at ambient temperature, and of the above modulability of its electronic properties. In particular, in the last two decades, some of us have developed, characterized and/or tested many advanced ferrocene derivatives [60,62,63], including planar-stereogenicity

ferrocenes for stereoselective catalysis applications (e.g. [74,75]). For example, the stereopure phosphinoferrocene ( $S_p$ )- $[\text{Fe}(\eta^5\text{-C}_5\text{H}_3\text{-1-PPh}_2\text{-2-(E)-CH=CHPh})(\eta^5\text{-C}_5\text{H}_5)]$  was employed as a ligand in palladium-catalyzed synthesis of sterically congested biaryls *via* Suzuki-Miyaura C,C cross-coupling reactions. [75] They have also formerly been applied in enantioselective allylic alkylations by P. Štěpnička *et al.* [77] To modulate the functional properties of this important parent molecule diverse modifications have been carried out. [74]

A wide systematic selection of the latter, with the phosphane groups protected as sulphides, is now submitted to a detailed electrochemical investigation (Table 1). Oxidation of the lone pair with chalcogenes is essential in order to prevent oxidation or dimerization processes. [79-81] Usage of  $\text{P}^V$ -sulfides is preferable, since oxidation of the ferrocenyl backbone can be excluded even though an excess of  $\text{S}_8$  is used (contrary to  $\text{H}_2\text{O}_2$ ), and also results in reversible redox processes, which is not ensured for the respective selenides. [79-81] Furthermore, selected compounds **1,5,7,14,15,16** (Table 1) are tested as planar stereogenicity model cases in voltammetric enantio-discrimination experiments, to achieve verification of the full-scope effectiveness of inherently chiral selectors in chiral electroanalysis.

**Table 1.** Electrochemical characterization of planar stereogenicity ferrocenes as racemates: a synopsis of key CV features in  $\text{CH}_3\text{CN} + 0.1 \text{ M} [\text{NBu}_4][\text{PF}_6]$  medium, including formal first oxidation potentials (related to the ferrocene site)  $E^{\circ}_{\text{Fc}}$ , first oxidation and reduction peak potentials,  $E_{\text{ia}}$  and  $E_{\text{ic}}$  respectively, oxidation and reduction peak potentials for the subsequent redox processes,  $E_{\text{Ia,IIa}}$  and  $E_{\text{Ic,IIc}}$ . All potentials are referred to the formal potential of the  $\text{Fc}^+/\text{Fc}$  couple measured in the same conditions. Highlighted are the compounds selected for the enantiodiscrimination tests. <sup>a</sup>[86], in  $\text{CH}_2\text{Cl}_2$ . <sup>b</sup>[86], in  $\text{CH}_3\text{CN}$ . <sup>c</sup>[87], in  $\text{CH}_2\text{Cl}_2$ . <sup>d</sup>[87], in  $\text{CH}_3\text{CN}$ . <sup>e</sup>[74], in  $\text{CH}_2\text{Cl}_2$ .

Compound	$\sigma^{[51]}$	$E^{\circ}_{\text{Fc}}$	$E_{\text{Ic,IIc}}$	$E_{\text{ic}}$	$E_{\text{ia}}$	$E_{\text{Ia,IIa}}$
	I			-2.90	1.18	1.42
	II	$\text{S=PPh}_2$ : $\sigma_p=0.47$	0.248 <sup>a</sup>			
	III	$\text{PPh}_2$ : $\sigma_p=0.19$ $\text{Fc}$ : $\sigma_p=$ $-0.18/-0.15$	0.064 <sup>a</sup> <b>0.080</b> <sup>b</sup> 0.101 <sup>c</sup> <b>0.097</b> <sup>d</sup>			
	1	Styr: $\sigma_p=-0.07$	<b>0.227</b> (0.200 <sup>e</sup> )	-2.93 -3.07	-2.69	0.26 1.17
	2	OMe: $\sigma_p=-0.27$	<b>0.188</b> (0.165 <sup>e</sup> )	-3.10	-2.81	0.22 0.87, 1.20
	3	Me: $\sigma_p=-0.17$	<b>0.216</b> (0.180 <sup>e</sup> )	-3.07	-2.75	0.26 1.22
	4	Cl: $\sigma_p=0.23$	<b>0.240</b> (0.210 <sup>e</sup> )	-3.08	-2.52 -2.71	0.28 1.16
	5	CN: $\sigma_p=0.66$	<b>0.267</b> (0.260 <sup>e</sup> )	-2.88 -3.03	-2.32 -2.49	0.30 1.25, 1.52

	6	CHO: $\sigma_p = 0.42$	<b>0.250</b> (0.245 <sup>e</sup> )	-3.08	-2.22 -2.51 (-2.41 <sup>sh</sup> )	<b>0.28</b>	1.32
	7	Styr: $\sigma_p = -0.07$	<b>0.180</b>	-3.12	-2.64 -2.79	<b>0.22</b>	<b>0.91, 1.23</b>
	8	SiMe <sub>3</sub> : $\sigma_p = -0.07$	<b>0.223</b>	-2.91 -3.02	-2.69	<b>0.26</b>	1.27
	9	SiEt <sub>3</sub> : $\sigma_p = -0.07$	<b>0.226</b>	-2.88	-2.68	<b>0.26</b>	1.27
	10	CH <sub>2</sub> OH: $\sigma_p = 0$	<b>0.169</b>	-3.21	-3.04	<b>0.20</b>	1.37
	11	CHO: $\sigma_p = 0.35$	<b>0.494</b>	-3.39	-2.44	<b>0.55</b>	<b>0.79, 1.20</b>
	12	Me: $\sigma_p = -0.17$	<b>0.219</b>	-3.48	-2.75	<b>0.25</b>	1.24
	13	Cl: $\sigma_m = 0.37$	<b>0.257</b>	-3.45	-2.56 -2.72	<b>0.29</b>	1.24
	14	CN: $\sigma_p = 0.66$	<b>0.281</b>	-2.86 -3.12	-2.20 -2.48	<b>0.32</b>	1.29
	15	cyclohexyl $\sigma_p = -0.15$	<b>0.185</b>	-3.57	-2.82	<b>0.23</b>	1.23
	16	Furyl $\sigma_p = 0.02/0.06$	<b>0.231</b>	-2.98 -3.14	-2.74	<b>0.27</b>	1.26

## Results and Discussion

### Synthesis

All compounds were synthesized according to previously reported procedures,<sup>[81-85]</sup> starting from ferrocenyl aldehydes, which were (stereo-)selectively lithiated in *ortho*-position followed by reaction with the appropriate phosphorus electrophile. The various vinyl functionalities were introduced using Horner-Wadsworth-Emmons (HWE) reactions of ferrocenyl aldehydes with phosphonates. Oxidation of the P<sup>III</sup> into the respective P<sup>V</sup> sulphides was performed by stirring of the parent compound with elemental sulphur. Substituents in 1'-position were introduced as described recently. For further details see the Experimental Section and the Supporting Information (section SI.2).

### Electrochemical investigation of the planar chiral ferrocenyl family as racemates

The series of chiral ferrocene racemates shown in Table 1 was investigated electrochemically, including both oxidative

and reductive features. The chosen measurement conditions were 0.1 M [NBu<sub>4</sub>][PF<sub>6</sub>] in acetonitrile as the supporting electrolyte, which is an appropriate medium for the subsequent enantiodiscrimination experiments on electrodes modified with oligo-(S<sub>a</sub>)-BT<sub>2</sub>T<sub>4</sub> films (see below). In contrast, dichloromethane, while resulting in easier ferrocene compound solubility, would be less convenient for operating the oligo-(S<sub>a</sub>)-BT<sub>2</sub>T<sub>4</sub> films on account of lower stability of the latter.<sup>[41]</sup> Moreover, it would prevent observation of the reductive features, on account of CH<sub>2</sub>Cl<sub>2</sub> reduction at relatively mild potentials. Key parameters of the CV patterns (reported as a gallery in SI. 4) are summarized in Table 1. For comparison, data are also provided for a series of first oxidation formal potentials formerly observed in CH<sub>2</sub>Cl<sub>2</sub> for compounds **1-6**<sup>[74]</sup>, as well as for triphenylphosphane sulphide (**I**) and diphenylferrocenylphosphane sulphide (**II**)<sup>[86]</sup> together with its parent P<sup>III</sup>-derivative **III**<sup>[86,87]</sup>, in CH<sub>3</sub>CN and/or CH<sub>2</sub>Cl<sub>2</sub>.<sup>[74]</sup> Relevant values of Hammett's constants<sup>[88]</sup> are also included.

### Oxidation

In most cases, except for aldehyde **11**, the first oxidation pro-

cess appears electrochemically reversible or quasi reversible, since peak potentials are nearly constant with increasing scan rate (details in SI.4) pointing to facile electron transfer. Moreover, such peaks correspond to single electron processes (considering half-peak widths) and are chemically reversible. Accordingly, Table 1 provides both peak potentials ( $E_{IA}$ ) and formal potentials ( $E^{o}_{Fc}$ ), the latter calculated as the average of forward and backward peaks. The peak features and the small slopes of the linear trends in systematic series of formal potentials with Hammett's  $\sigma$  parameters (Figure 3), pointing to a significant distance between substituent and redox site, are consistent with the first oxidation involving the ferrocene site. While switching to  $\text{CH}_2\text{Cl}_2$  as working medium (orange series, in Figure 3) results in a linear fit similar to one for  $\text{CH}_3\text{CN}$ , but with higher slope, consistently with the lower solvent shielding effect.

strong electron-withdrawing character of the formyl functionality ( $\sigma_p = 0.42$ ). Moreover, the peak appears nearly chemically irreversible, pointing to a chemical follow up reaction, the only case in the series, which could be justified by the much more positive potential and/or by some involvement of the aldehyde group besides the ferrocene one (although oxidation of the formyl group could correspond to the second oxidation peak at 0.79 V). Anisyl derivative **2** also exhibits a further redox process, observed at 0.87 V, most likely occurring at the methoxyphenyl group. The 1'-functionalized ferrocene **7**, bearing two phenyl vinyl functionalities, shows a process at 0.91 V, for which an intramolecular  $\pi$ -stacking might be involved. All compounds exhibit a further process at  $\sim 1.2$  V vs  $\text{Fc}^+|\text{Fc}$  which closely matches the oxidation peak potential of  $\text{S}=\text{P}(\text{Ph})_3$  itself (Table 1 and SI.4 section in SI).

### Reduction

Unlike the first oxidation peaks, first reduction events appear chemically irreversible and, in most cases, also electrochemically irreversible. However, they also can be correlated in systematic sequences in terms of potential vs  $\sigma$  linear regressions (Figure 3). For instance, for the series with different substituents on the styryl group (parent **1** plus **2–6**) a linear Hammett plot is observed (Figure 3 top). Compared with the correlation of the first oxidation peaks, the slope is much higher, pointing to first reductions taking place in proximity of, or directly at, the respective phenyl substituent. This assumption is also supported by the peculiar two-peak reduction patterns observed for specific cases like **4** (chlorophenyl substituent) and **6** (acyl substituent). In particular, in the first case first reduction must correspond to the carbon-chloride reductive cleavage<sup>[89]</sup>, while in the second case it should be mostly centered on the formyl group, a feature that would justify why the acyl derivative **6** does not correlate with the Hammett plot of the related compounds **2–5** (Figure 3 top).

It is worthwhile noticing that the reduction potentials appear by far less negative than the corresponding simple substituted benzenes (for example, benzonitrile reduction takes place at about  $-2.8$  V vs  $\text{Fc}^+|\text{Fc}$  on GC in  $\text{CH}_3\text{CN}$  +  $0.1$  M  $[\text{NEt}_4][\text{BF}_4]$ <sup>[90]</sup>), as reasonable considering that in this case the benzene ring is part of an extended conjugated system, including the double bond and the ferrocene ring itself, bearing the highly electron attracting P=S group. Concerning reduction of the phosphane sulphide group, it might correspond to the second reduction peak system, falling in the range between  $-2.88$  V and  $-3.10$  V (Table 1), which is similar to triphenyl phosphane sulphide itself ( $-2.9$  V vs  $\text{Fc}^+|\text{Fc}$ ).

Figure 3 (top) also includes the three cases of functionalization on the second cyclopentadienyl ring. While the presence of trialkylsilyl groups in 1' position (**8,9**) is practically unperceivable in respect to the parent case, consistent with a Hammett constant close to zero, a styrene group (**7**) results in a more positive reduction peak and a more negative oxidation peak (*i.e.* both easier oxidation and reduction), which can be justified in terms of a mesomeric effect as a result of extended conjugation, possibly also via  $\pi$  stacking. This might also explain the double peak system (see SI 2), which might account for two near-equivalent redox

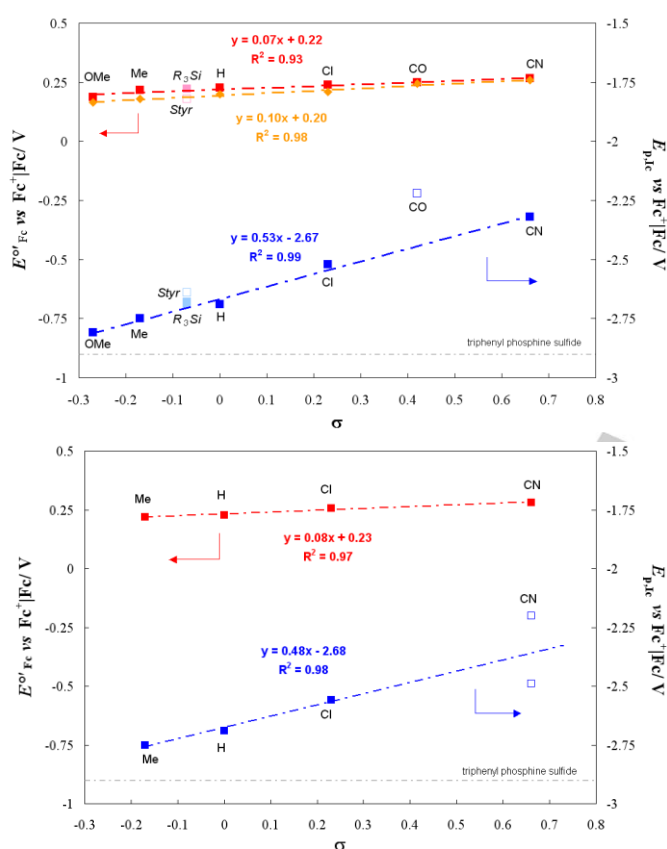


**Figure 3.** Hammett relationships for the formal first (ferrocenyl-based) oxidation potentials  $E^{o}_{Fc}$  (red) and the first reduction peak potentials  $E_{ic}$  (blue) of a series of planar stereogenicity chiral ferrocenes. Top: altering the substituents on the phenyl ring of the styrene system (**1**, **2–6**, upright characters) and 1'-substituted ferrocenyl derivatives (**7–9**, italic characters). Bottom: altering the substituents of the phenyl groups in the phosphinyl moiety (**1**, **12–14**).

The peak potential values of 0.22–0.32 V vs unsubstituted  $\text{Fc}^+|\text{Fc}$  are quite justified by the presence of the highly electron withdrawing  $\text{P}^{\text{V}}$  group  $\text{S}=\text{PPh}_2$  ( $\sigma_p = 0.47$ ) compared to  $\text{P}^{\text{III}}$  in  $\text{PPh}_2$  ( $\sigma_p = 0.19$ ), whereby the weakly electron donating styrene group is less determining ( $\sigma_p = -0.07$ ). The only exception is observed for aldehyde **11**, displaying an electrochemically irreversible behavior. The first oxidation process is anodically shifted to 0.49 V vs  $\text{Fc}^+|\text{Fc}$ , due to the

centres (*i.e.* the two styrene-cyclopentadienyl moieties) reciprocally interacting, although the presence of the electron attracting phosphane sulphide on one of the conjugated systems may also contribute to the potential difference.

Similarly, changing the substituents on the phenyl groups on the phosphane sulphide site (parent **1** plus **12–14**, Figure 3 bottom), dominantly impacts the reduction potentials (higher slope in the Hammett correlation), whereas the ferrocenyl-based oxidation process is far less affected. This suggests that in this sub-series, the first reduction process moves on the thiophosphinyl groups, in particular the aryl substituents. Notably, the reduction potentials are very similar to the former series. In this case, the positive shifts of the reduction potentials, with respect to simple substituted benzenes, can be justified by the adjacent electron attracting phosphane sulphide group. Again, the expected complex pattern starting with C–Cl bond cleavage is observed for chlorophenyl group reduction in **13**. The two reversible one-electron peak systems observed in the cyanophenyl case **14** might point to a couple of equivalent interacting redox sites, namely the two *gem-p*-CN-C<sub>6</sub>H<sub>4</sub> substituents of the phosphane sulphide. This hypothesis could also explain why the Hammett correlation is intermediate between the two first reduction peak potentials.

In case of non-substituted phenyl rings (**1**), the challenge is to understand the reduction sequence between, on one side, the phosphane sulphide site, and on the other side the phenyl terminal of the opposite styryl conjugated system. Taking triphenyl phosphane sulphide (**1**) as benchmark for the electrochemical activity of the P=S group ( $E_{P,ic} = -2.90$  V vs Fc<sup>+</sup>/Fc, Table 1), and considering that addition of the weakly electron donating ferrocenyl substituent could result in a negative shift of the signal, we assume the first reduction peak of the ferrocene derivatives (more positive than  $-2.82$  V vs Fc<sup>+</sup>/Fc for all styryl-bearing compounds, Table 1) to correspond to an aromatic group rather than to P=S reduction. *Vice versa*, phenyl group reduction, usually located at more negative potentials, as above mentioned, could be promoted in the present compounds, either, on one molecule side, by the strongly electron attracting character of the phosphane sulphide group or, on the other side, by extended  $\pi$  conjugation (also evident in the case of an analogous compound with a ferrocenyl group replacing the phenyl one in the styryl system<sup>[74]</sup>). Actually, the parent compound **1** appears to fit on both Hammett correlations together with substituted relatives (**12–14** in one case, **2–6** in the other case). Thus, first reduction could indeed involve a phenyl ring; to decide which one, it is interesting to note that:

*i*) replacement of phenyl by furyl substituents (compare **1** to **16**) only results in slight changes in the CV pattern on both sides;

*ii*) changing from aromatic to aliphatic phosphane sulphide substituents (compare **1** with **15**), the second reduction system at  $-2.93$  V disappears. Thus it should correspond to the reduction of the phenyl groups on the phosphane sulphide site, while the first reduction peak at  $-2.82$  V, still consistent with the Hammett straight line, should correspond to the reduction of the phenyl group of the styrene moiety. Thus, the second reduction of **15** at  $-3.57$  V should correspond to the reduction of the alkyl phosphane sulphide group, which could be significantly less favoured with respect to the aryl case

consistently with the well-known higher oxidability of alkyl phosphanes compared to aryl ones.

*iii*) Replacing the styryl moiety with an hydroxymethyl one (compound **10**), locates the first reduction peak at  $-3.04$  V, very close to prototypical triphenylphosphane sulphide  $-2.90$  V. *Vice versa*, a formyl group in the same position (compound **11**) results in a remarkable positive shift of the first reduction ( $-2.44$  V), since the process specifically concerns the aldehyde group.

In conclusion, the above clues point to consider the phenyl unit of the styrene moiety as the most easily reducible site ( $-2.7$  V vs Fc<sup>+</sup>/Fc) in the prototype **1**.

Concerning interpretation of the phenyl sulphide group reduction, a puzzling feature is the splitting observed in many cases for the second reduction peak, which might even account for interacting redox centers (the aryl substituents), but is hard to analyze, being so close to the background.

Among the investigated racemic ferrocenes, we have carefully selected six terms to be separated by preparative chiral HPLC and employed as model probes for the enantio-selection voltammetry tests: **1**, the parent compound; **5** and **14**, to evaluate the effect of the same substituent in the styrene vs the phosphane sulphide moiety (notably -CN, also potentially acting as valuable coordination site in stereoselective analysis and catalysis); **16**, to compare heteroaromatic vs aromatic phosphane sulphide substituents; **15**, to compare aliphatic vs aromatic phosphane sulphide substituents; and **7**, a case in which the styrene units could be reciprocally engaged in  $\pi$ -stacking.

#### Separation of the ferrocenyl chiral probes into pure enantiomers by chiral HPLC

The chromatographic enantioseparations of the chiral ferrocenes were carried out using the polysaccharide-based Chiralpak IG-3 CSP in combination with normal-phase eluents. In the Chiralpak IG-3 CSP the chiral selector amylose tris(3-chloro-5-methylphenylcarbamate) is immobilized onto 3  $\mu$ m particles of silica. Two types of binary mixtures were used as mobile phases, namely *n*-hexane/2-propanol 60:40 for the compounds **1**, **7**, **15**, **16**, and *n*-hexane/2-propanol 40:60 for **5** and **14**.

As shown in Figure 4 (left column) an excellent enantiomer separation was achieved in all cases, significantly modulated by the ferrocenyl substituents. Indeed the compound family can provide an attractive model case for a fundamental HPLC study concerning planar stereogenicity compounds, a topic so far surprisingly underexplored. The described process was scaled-up to a semipreparative level, where both enantiomers could be collected in multi-milligram quantities, by performing injections of about 10–20 mg of racemic samples on a 10-mm I.D. Chiralpak IG column. All enantio-separations were achieved in non-overlapping band conditions, and the analytical control of the collected fractions results in an *ee* of >99% for both enantiomers and excellent recovery rates between 90% and 95%.

In order to determine the enantiomer elution order, dichloromethane solutions of the collected enantiomers were submitted to circular dichroism (CD) analysis. As reported in Figure 4 (right column) the shape and the absorption maxima of the CD spectra of the first eluting enantiomers of chiral compounds are strictly correlated with those of the less retained

( $S_p$ )-enantiomer of **1** and **16**. For both, enantiopure samples could be used for comparison, synthesized according to a previously reported procedure.<sup>[77]</sup> Therefore, the empirical CD correlation method indicates that all ferrocene analogues studied exhibit the same sense of chiral recognition, and consequently the same enantiomer elution order on the Chiralpak IG CSP with preferential retention of the ( $R_p$ )-enantiomer.

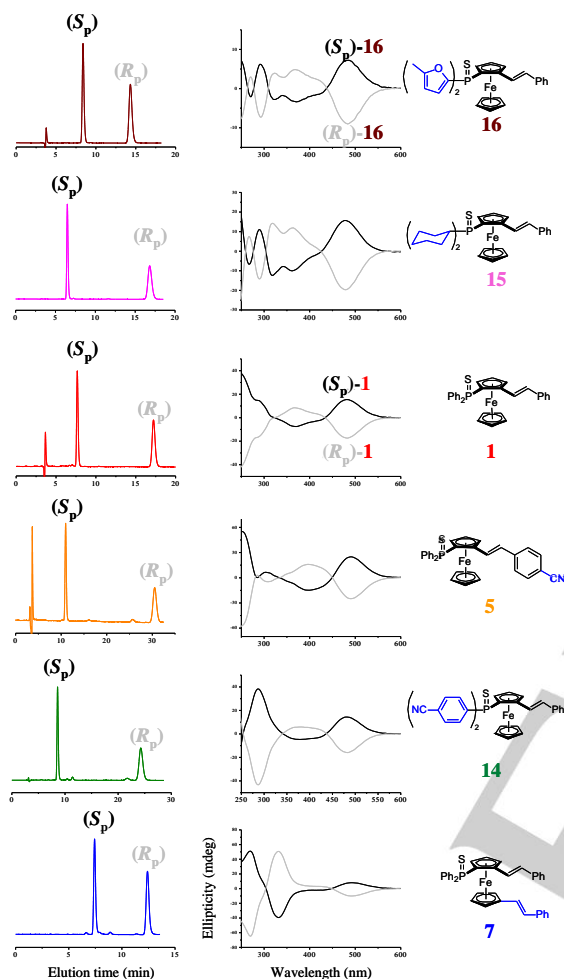


**Figure 4.** Chiral HPLC separation of the selected probes and circular dichroism spectra of the isolated fractions.

### Enantioselective recognition in CV experiments

The enantiopure antipodes of the six selected planar-stereogenic ferrocenes have been studied in CV experiments on a GC (GC = Glassy Carbon) electrode modified with inherently chiral electroactive oligo-(BT<sub>2</sub>T<sub>4</sub>) films, potentiodynamically electrodeposited in CH<sub>3</sub>CN solutions containing 0.1 M [NBu<sub>4</sub>][PF<sub>6</sub>] as supporting electrolyte along the protocol described in the Experimental Section. An example of CV patterns for both, electrodeposition and stability check, steps is reported in SI.5.

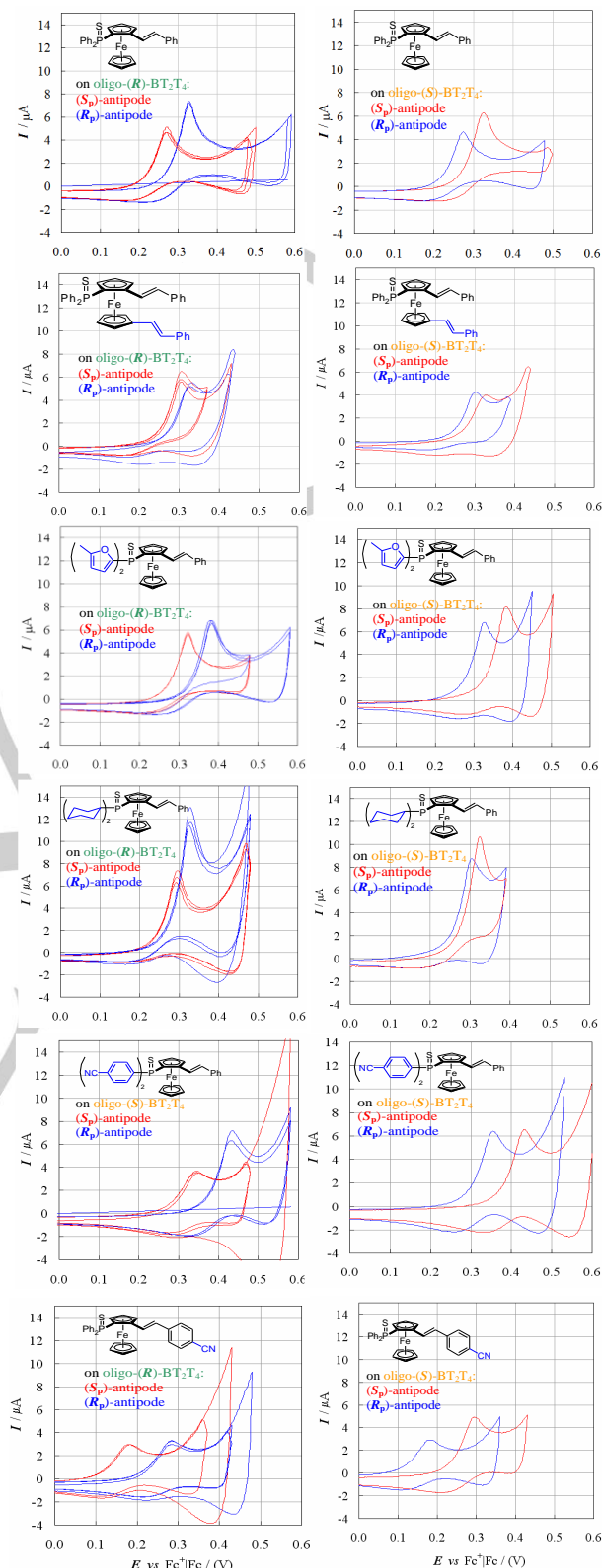


**Figure 5.** Enantiodiscrimination experiments with planar stereogenicity probes as enantiopure ( $S_p$ ) and ( $R_p$ ) antipodes. CV patterns on a GC electrode modified with oligo-( $R$ )-BT<sub>2</sub>T<sub>4</sub> films (left, also providing reproducibility tests as superimposed CV curves) and oligo-( $S$ )-BT<sub>2</sub>T<sub>4</sub> films (right).



Figures 5a and 5b provide a synopsis of the first oxidation CV peaks observed for the ( $S_p$ ) and the ( $R_p$ ) enantiomers (red and blue, respectively) of ferrocenes **1,5,7,14,15,16** selected as probes on oligo-( $R_a$ )-(BT<sub>2</sub>T<sub>4</sub>) (left column) and oligo-( $S_a$ )-(BT<sub>2</sub>T<sub>4</sub>) surfaces (right column).

Contrary to ( $S$ )-(-)- and ( $R$ )-(+)-*N,N*-dimethyl-1-ferrocenyl-ethylamine, a standard chiral ferrocenyl probe with central stereogenicity, which undergoes first oxidation well before the film oxidation, and usually results in (quasi) canonical, reversible peaks on oligo-(BT<sub>2</sub>T<sub>4</sub>) films [35,36,45], the first oxidation process of the planar-stereogenicity probes is shifted to the onset of the film oxidation, on account of the highly electron attracting phosphane sulphide substituent, as discussed earlier. This can justify the irreversible, non-canonical first oxidation peak shape, quite different from the bare electrode case. Actually, the ferrocenyl-based oxidation process also appears to have some effect on the film oxidation onset, which is usually very reproducible, while it shows significant differences in the considered cases.

Nevertheless, a significant peak potential difference is observed for the two enantiomers in all the six probe cases, neatly specular upon inverting either probe or surface configuration.

In particular, specular (*i.e.*, energetically equivalent) combinations **A** ( $S_p$ )-probe+( $R_a$ )- and ( $R_p$ )-probe+( $S_a$ )-selector, respectively, have their first oxidation at a less positive potential with respect to specular combinations **B** ( $R_p$ )-probe+( $R_a$ )- and ( $S_p$ )-probe+( $S_a$ )-selector. Actually, the **A** and **B** combination couples are reciprocally in a diastereomeric relationship, which implies an energy difference, which is affected by the probe substituents.

Notably, the same sequence of configuration combinations applies to all the six selected cases; thus, the considered structural and electronic modifications in respect to the parent molecule **1** do not basically alter the probe-selector configurational matching. However, they appear to remarkably modulate the energy difference between the **A** and **B** diastereomeric couples. In particular, taking as benchmark the CV patterns of the parent probe **1** enantiomers (couples **A** at  $\sim 0.27$  V; couples **B** at  $\sim 0.33$  V;  $\sim 50$  mV separation),

- in the furyl case **16** the peak difference is only slightly higher (couples **A** at  $\sim 0.32$  V; couples **B** at  $\sim 0.38$  V;  $\sim 60$  mV separation)
- the peak difference is significantly narrower in the cyclohexyl derivative **15** (couples **A** at  $\sim 0.30$  V; couples **B** at  $\sim 0.33$  V;  $\sim 30$  mV separation) and in the double styrene case **7** (couples **A** at  $\sim 0.30/31$  V; couples **B** at  $\sim 0.33$  V;  $\sim 20/30$  mV separation);
- conversely, the peak difference is remarkably larger in both nitrile cases. Compound **14**: couples **A** at  $\sim 0.35/0.36$  V; couples **B** at  $\sim 0.43/0.44$  V;  $\sim 70/90$  mV separation. Compound **5**: couples **A** at  $\sim 0.18$  V; couples **B** at  $\sim 0.28/0.30$  V;  $\sim 100/120$  mV separation.

Actually, assuming probe-selector matching elements to consist i) on the conjugated systems (with related  $\pi$  conjugation/stacking effects), and ii) on the heteroatoms (with related lone pair availability), both largely present in our model cases, and strictly related to the stereogenic elements, the above listed peak differences could be justified as follow:

- the number of available matching elements decrease changing the phenyl substituents (parent compound **1**) into alkyl ones (compound **15**);
- according to the above assumed engagement of both styrene groups in reciprocal  $\pi$  interaction in compound **7**, the availability of these groups for chiral matching should be much lower in **7** respect to **1**;
- conversely the nitrile substituents in **5** and **14** provide powerful additional matching elements (particularly effective in **5**, maybe on account of higher availability). Also the slight improvement observed with furyl blades (in **16**) might be related to the additional heteroatoms.

## Conclusion

Sixteen planar-stereogenicity ferrocenes, important *e.g.* as chiral ligands in stereoselective catalysis, are here characterized in terms of relationships between structure and electronic properties, including reduction processes, usually neglected in this compound family. For a rationally selected group, enantiopure antipodes are obtained by semipreparative chiral HPLC separation and eventually successfully discriminated by oligo-BT<sub>2</sub>T<sub>4</sub> inherently chiral electrodes, in terms of significant potential differences, specular inverting probe or selector configuration, pointing to significant energy differences between diastereomeric probe-selector combinations. Substituent changes do not alter the enantiomer peak sequence, neither in HPLC elution nor in electrochemical tests, but significantly modulate the peak potential difference between antipodes of the same probe in the potentiodynamic scans, in a way which appears consistent with the availability of chiral/selector matching elements.

The general effectiveness of inherent chirality selectors is thus confirmed, since it also applies to planar stereogenicity probes. As an additional bonus, the chosen systematic case series suggested attractive clues on the matching elements involved in the enantiorecognition process. Indeed planar stereogenicity ferrocenes are outstanding models for enantiodiscrimination mechanistic studies, in both voltammetry and chromatography, worthy of further investigations, both widening the model case series and in synergy with computational and chiroptical approaches.

## Experimental Section

### Synthesis.

The parent P<sup>III</sup> phosphines of compounds **1**,<sup>[75]</sup> **2-6,12-13,15,16**,<sup>[74]</sup> **7-9,14,16**<sup>[82]</sup> and **10,11**<sup>[83-85]</sup> were synthesized according to published procedures. The herein applied P<sup>V</sup>-sulphides were obtained by stirring of the parent P<sup>III</sup> phosphines with an excess of elemental sulphur in dichloromethane or tetrahydrofuran according to literature.<sup>[74,80]</sup> The synthesis of the hitherto not reported compounds **7-9** is given in the Supporting Information. Compound **1** is commercially available (Sigma Aldrich).

### Chiral HPLC.

The HPLC apparatus used for analytical enantioseparations consisted of a PerkinElmer (Norwalk, CT, USA) 200 LC pump equipped with a Rheodyne (Cotati, CA, USA) injector, a 50  $\mu$ L sample loop, an HPLC

PerkinElmer oven and a PerkinElmer detector. The signal was acquired and processed by Clarity software (DataApex, Prague, Czech Republic). In analytical separations, fresh standard solutions of racemic samples were prepared shortly before using by dissolving about 1 mg of analyte in 10 mL of mobile phase. The injection volume was 20  $\mu$ L.

For semi-preparative separation, a PerkinElmer 200 LC pump equipped with a Rheodyne injector, a 5000  $\mu$ L sample loop, a PerkinElmer LC 101 oven and Waters 484 detector (Waters Corporation, Milford, MA, USA) was used. The feed solution for milligram-scale enantioseparations was prepared by dissolving 10-20 mg of racemic ferrocenes in 1 mL of acetone and diluting the solution with 4 mL of mobile phase.

#### Electrochemistry

Cyclic voltammetry experiments were performed using an Autolab PGSTAT potentiostat (Eco-Chemie, Utrecht, The Netherlands), controlled by a PC with the GPES software provided by the same manufacturer. The three-electrode V-shaped minicell (with 3 cm<sup>3</sup> of solution) included a glass-embedded glassy carbon disk (GC, Metrohm, S = 0.033 cm<sup>2</sup>) as working electrode, a Pt disk as counter electrode, and an aqueous saturated calomel (SCE) as reference electrode, inserted in a compartment filled with the working medium and ending with a porous frit, to avoid water and KCl leakage into the working solution. The optimized preliminary polishing procedure for the GC disk electrode consisted in treatment with a diamond powder of 1  $\mu$ m diameter (Aldrich) on a wet DP-Nap cloth (Struers).

The characterizations of the ferrocene derivatives as racemates were performed at scan rates in the 0.02-2 V/s range, on 0.001-0.0005 M probe solutions in acetonitrile, CH<sub>3</sub>CN (Aldrich, HPLC grade), with 0.1 M tetrabutylammonium hexafluorophosphate (NBu<sub>4</sub>PF<sub>6</sub>) as supporting electrolyte (Fluka,  $\geq$ 98 %), applying ohmic drop compensation by the positive feedback method and referring the potentials to the Fc<sup>+</sup>/Fc redox couple (the intersolvental standard recommended by IUPAC [23]) measured in the same conditions (~0.39 V vs SCE).

Electrodepositions of conducting chiral (*R*<sub>a</sub>)-oligo-BT<sub>2</sub>T<sub>4</sub> and (*S*<sub>a</sub>)-oligo-BT<sub>2</sub>T<sub>4</sub> films were performed by repeated 36 CV cycles at 0.05 V/s scan rate on the GC disk electrode with 0.00075 M solutions of the corresponding enantiopure (*R*<sub>a</sub>)- or (*S*<sub>a</sub>)-BT<sub>2</sub>T<sub>4</sub> monomer, in CH<sub>3</sub>CN with 0.1 M NBu<sub>4</sub>PF<sub>6</sub> supporting electrolyte. The enantio-discrimination experiments were performed with enantiopure chiral probes **1,5,7,14,15,16** at 0.05 V/s scan rate in 0.001 M solutions of the probe in CH<sub>3</sub>CN + NBu<sub>4</sub>PF<sub>6</sub> 0.1 M as supporting electrolyte. Reproducibility tests were performed by repeatedly recording the CV patterns of model probes on freshly deposited chiral surfaces.

## Acknowledgements

The Authors are grateful to Professor Francesco Sannicolò (Laboratori Alchemia, Milano) for discussion, suggestions, and precious help in the formulation of the stereogenicity/chirality concepts. Financial support of Fondazione Cariplo and Regione Lombardia (2016-0923 RST-Avviso congiunto FC-RL Sottomisura B) rafforzamento (Enhancing VINCE (Versatile INherently Chiral Electrochemistry)) is gratefully acknowledged.

**Keywords:** enantiodiscrimination in electroanalysis; chiral electrodes; chiral voltammetry; electroactive probes of chiral planarity; electrode surface modification with inherently chiral electroactive oligomers; 1,2-planar-chiral alkenylferrocenyl phosphanes of catalytic interest.

- [1] S. Mane, *Anal. Methods* **2016**, *8*, 7567-7586.
- [2] S. Arnaboldi, M. Magni, P. Mussini, *Curr. Opin. Electrochem.* **2018**, *8*, 60-72.
- [3] S. Arnaboldi, S. Grecchi, M. Magni, P. Mussini, *Curr. Opin. Electrochem.* **2018**, *7*, 188-199.
- [4] F. Pop, N. Zigon, N. Avarvari, *Chem. Rev.*, **2019**, *119*, 8435-8478
- [5] E. Zor, H. Bingol, M. Ersoz, *Trends Anal. Chem.* **2019**, *121*, 115662
- [6] C. Wattanakit, A. Kuhn, *Chem. Eur. J.*, **2020**, *26*, 2993-3003

- [7] R. A. Zilberg, V. N. Maistrenko, L. R. Kabirova, D. I. Dubrovsky, *Anal. Methods*, **2018**, *10*, 1886-1894
- [8] Z. Li, Z. Mo, P. Yan, S. Meng, R. Wang, X. Niu, N. Liu, R. Guo, *New J. Chem.*, **2018**, *42*, 11635-11641
- [9] L. Zhang, G. Wang, C. Xiong, L. Zheng, J. He, Y. Ding, H. Lu, G. Zhang, K. Cho, L. Qiu, *Biosens. Bioelectron.* **2018**, *105*, 121-128
- [10] L. Zhang, Z. Liu, C. Xiong, L. Zheng, Y. Ding, H. Lu, G. Zhang, L. Qiu, *Org. Electron.* **2018**, *61*, 254-260
- [11] S. S. Upadhyay, A. K. Srivastava, *New J. Chem.*, **2019**, *43*, 11178-11188
- [12] X. Niu, Z. Mo, H. Gao, R. Wang, Z. Lim S. Meng, R. Guo, *J. Solid State Electrochem.* **2018**, *22*, 973-981
- [13] C. Pu, Y. Xu, Q. Liu, A. Zhu, G. Shi, *Anal. Chem.* **2019**, *91*, 4, 3015-3020
- [14] L. Dong, X. Liu, H. Xu, D. Wu, S. Gao, L. Zhong, Y. Kong, *Chirality*, **2019**, *31*(11), 917-922
- [15] X. Niu, X. Yang, Z. Mo, R. Guo, N. Liu, P. Zhao, Z. Liu, *Bioelectrochemistry*, **2019**, *129*, 189-198
- [16] J. Yang, D. Wu, G.-C. Fan, L. Ma, Y. Tao, Y. Quin, Y. Kong, *Electrochem. Comm.* **2019**, *104*, 106478
- [17] S. Assavapanumat, M. Ketkaew, A. Kuhn, C. Wattanakit, *J. Am. Chem. Soc.*, **2019**, *141*, 18870-18876
- [18] S. Assavapanumat, B. Gupta, G. Salinas, B. Goudeau, C. Wattanakit, A. Kuhn, *Chem. Commun.*, **2019**, *55*, 10956-10959
- [19] G. Zhu, D. Zhang, Y. Ma, Y. Yi, *J. Electrochem. Soc.*, **2020**, *167*, 027523.
- [20] T. S. Metzger, S. Mishra B. P. Bloom, N. Goren, A. Neubauer, G. Shmul, J. Wie, S. Yochelis F. Tassinari, C. Fontanesi, *Angew. Chem. Int. Ed.*, **2020**, *59*(4), 1653-1658
- [21] K. Naveen, H. Lee, D. Lee, J. Jun Lee, J. Min Moon, Y. Shim, O. Jung, *Cryst. Growth Des.* **2018**, *18*, 10, 6266-6272
- [22] M. Gazzotti, S. Arnaboldi, S. Grecchi, R. Giovanardi, M. Cannio, L. Pasquali, A. Giacomino, O. Abollino, C. Fontanesi, *Electrochim. Acta* **2018**, *286* 271-278
- [23] D. Wu, W. Tan, Y. Yu, B. Yang, H. Li, Y. Kong, *Anal. Chim. Acta*, **2018**, *1033*, 58-64
- [24] W. Liang, Y. Rong, L. Fan, W. Dong, Q. Dong, C. Yang, Z. Zhong, C. Dong, S. Shuang, W.-Y. Wongm J. Mater. Chem. C, **2018**, *6*, 12822
- [25] D. Wu, F. Pan, G. C. Fan, Z. Zhu, L. Gao, Y. Tao, Y. Kong, *Analyst*, **2019**, *144*, 6415-6421.
- [26] Z. Li, H. Xu, D. Wu, J. Zhang, X. Liu, S. Gao, Y. Kong, *ACS Appl. Mater. Interfaces* **2019**, *11*, 3, 2840-2848
- [27] B. Liu, H. Lian, L. Chen, X. Wei, X. Sun, *Anal. Biochem.*, **2019**, *574*, 39-45
- [28] J. Zou, J.-G. Yu, *Anal. Chim. Acta*, **2019**, *1088*, 35-44
- [29] A. Stoian, I. Bogdan-Cezar, João P. Prates, Ramalho, I. Ovidiu Marian, C. Vasile, E. Bodoki, R. Oprean, *Electrochim. Acta*, **2019**, *326*, 134961.
- [30] S.-Y. Wang, L. Li, Y. Xiao, Y. Wang, *Trends Analyt. Chem.*, **2019**, *121*, 115691
- [31] J. Guo, X. Wei, H. Lian, L. Li, X. Sun, B. Liu, *ACS Appl. Nano Mater.* **2020**, *3*, 4, 3675-3683
- [32] D. Kim, K.-D. Seo, D. Moon, Y.-B. Shim, S.H. Lee, O.-S. Jung, *Inorg. Chem.* **2020**, *59*, 9, 5808-5812
- [33] Y-x. Sun, J.-h. He, J.-w. Huang, Y. Sheng, D. Xu, M. Bradley, R. Zhang, *J. Electroanal. Chem.* **2020**, *865*, 114130
- [34] R. A. Zilberg, V. N. Maistrenko, L. R. Zagitova, V. Y. Guskov, D. I. Dubrovsky, *J. Electroanal. Chem.*, **2020**, *861*, 113986
- [35] F. Sannicolò, P. R. Mussini, T. Benincori, R. Cirilli, S. Abbate, S. Arnaboldi, S. Casolo, E. Castiglioni, G. Longhi, R. Martinazzo, M. Panigati, M. Pappini, E. Quartapelle Procopio, S. Rizzo, *Chem. Eur. J.* **2014**, *20*, 15298-15302.
- [36] F. Sannicolò, S. Arnaboldi, T. Benincori, V. Bonometti, R. Cirilli, L. Dunsch, W. Kutner, G. Longhi, P. R. Mussini, M. Panigati, M. Pierini, S. Rizzo, *Angew. Chem. Int. Ed.* **2014**, *53*, 2623-2627
- [37] S. Arnaboldi, T. Benincori, R. Cirilli, W. Kutner, M. Magni, P.R. Mussini, K. Noworyta, F. Sannicolò, *Chem. Sci.* **2015**, *6*, 1706-1711.

- [38] S. Arnaboldi, T. Benincori, R. Cirilli, S. Grecchi, L. Santagostini, F. Sannicolò, P. R. Mussini, *Anal. Bioanal. Chem.* **2016**, 408, 7243–7254.
- [39] F. Sannicolò, P. R. Mussini, T. Benincori, R. Martinazzo, S. Arnaboldi, G. Appoloni, M. Panigati, E. Quartapelle Procopio, V. Marino, R. Cirilli, S. Casolo, W. Kutner, K. Noworyta, A. Pietrzyk-Le, Z. Iskierko and K. Bartold, *Chem. Eur. J.* **2016**, 22, 10839 – 10847.
- [40] S. Arnaboldi, T. Benincori, A. Penoni, L. a Vaghi, R. Cirilli, S. Abbate, G. Longhi, G. Mazzeo, S. Grecchi, M. Panigati, and P. R. Mussini *Chem. Sci.*, **2019**, 2708-2717
- [41] S. Arnaboldi, S. Cauteruccio, S. Grecchi, T. Benincori, M. Marcaccio, A. Orbelli Biroli, G. Longhi, E. Licandro, P.R. Mussini, *Chem.Sci.*, **2019**, 6, 1706-1711.
- [42] S. Rizzo, S. Arnaboldi, V. Mihali, R. Cirilli, A. Forni, A. Gennaro, A. Ahmed Isse, M. Pierini, P. R. Mussini, F. Sannicolò, *Angew. Chemie* **2017**, 56, 2079-2082.
- [43] S. Rizzo, S. Arnaboldi, R. Cirilli, A. Gennaro, A. Ahmed Isse, F. Sannicolò, P. R. Mussini, *Electrochem. Comm.* **2018**, 89, 57-61
- [44] Results to be submitted for publication to *Anal. Chem.*
- [45] S. Arnaboldi, D. Vigo, M. Longhi, F. Orsini, S. Riva, S. Grecchi, E. Giacobelli, V. Guglielmi, R. Cirilli, G. Longhi, G. Mazzeo, T. Benincori, P.R. Mussini, *ChemElectroChem* **2019**, 6, 4204-4214.
- [46] J. Hrbac, V. Pavelka, J. Crassous, J. Zadny, L. Fekete, J. Pokorny, P. Vanysek, J. Storch, J. Vacek, *Electrochem. Comm.* **2020**, 113, 106689
- [47] Z. Hassan, E. Spuling, D. M. Knoll, J. Lahann, S. Bräse, *Chem. Soc. Rev.* **2018**, 47, 6947-6963
- [48] Y. Morisaki, Y. Chujo, *Bull. Chem. Soc. Jap.* **2019**, 92, 265-274.
- [49] M. Hasegawa, K. Kobayakawa, Y. Nojima, Y. Mazaki, *Org. Biomol. Chem.*, **2019**, 17, 8822
- [50] M. Bau, S. Wiesler, S.L. Younas, J. Streuff, *Chem. Eur. J.* **2019**, 25, 10531-10545.
- [51] F. Pop, N. Zigon, N. Avarvari, *Chem. Rev.* **2019**, 119, 8435-8478.
- [52] S. Fa, T. Kakuta, T. Yamagishi, T. Ogoshi, *Chem. Lett.* **2019**, 48, 1278-1287.
- [53] D. Marquading, H. Klusacek, G. Gokel, P. Hoffmann, I. Ugi, *J. Amer. Chem. Soc.* **1970**, 92, 5389-5393
- [54] K. Yoshida, R. Yasue, *Chem. Eur. J.* **2018**, 24, 18575-18586
- [55] D. Schaarschmidt, H. Lang, *Organometallics* **2013**, 32, 5668-5704
- [56] G. Gritzner, J. Kuta, *Pure Appl. Chem.* 1982, 54, 1527-1532
- [57] S.P. Gubin, *Russ. Chem. Bull.* **1966**, 15, 1495–1501
- [58] C. Baldoli, E. Licandro, S. Maiorana, D. Resemini, C. Rigamonti, L. Falcicola, M. Longhi, P. R. Mussini, *J. Electroanal. Chem.* **2005**, 585,197–205.
- [59] A. Mulas, Y. Willener, J. Carr-Smith, K. M. Joly, L. Male, C. J. Moody, S. L. Horswell, H. V. Nguyen, J. H. R. Tucker, *Dalton Trans.* **2015**, 44, 7268-7275.
- [60] A. Hildebrandt, D. Schaarschmidt, R. Claus, H. Lang, *Inorg. Chem.* **2011**, 50, 10623-10632.
- [61] F. Rose-Munch, M. Li, E. Rose, J. C. Daran, A. Bossi, E. Licandro, and P. R. Mussini, *Organometallics* **2012**, 31, 92–104.
- [62] U. Pfaff, A. Hildebrandt, D. Schaarschmidt, T. Rüffer, P. J. Low, H. Lang, *Organometallics* **2013**, 32, 6106–6117.
- [63] A. Hildebrandt, H. Lang, *Organometallics* **2013**, 32, 5640-5653.
- [64] T.J. Barton, I. N. Douglas, R. Grinter, A.J. Thomson, *J. Chem. Soc., Dalton Transactions* **1976**, 29, 2948-2954.
- [65] T. Benincori, S. Arnaboldi, M. Magni, S. Grecchi, R. Cirilli, C. Fontanesi, P. R. Mussini, *Chem. Sci.*, **2019**, 10, 2750-2757.
- [66] A. Togni, *Angew. Chem. Int. Ed.* **1996**, 35, 1475-1477
- [67] C. J. Richards, Andrew J. Locke, *Tetrahedron: Asymmetry* **1998**, 9, 2377-2407.
- [68] T. J. Colacot, *Chem. Rev.* **2003**, 103, 3103-3118
- [69] D. Li-Xin, T. Tao, Y. Shu-Li, D. Wei-Ping, H. Xue-Long *Acc. Chem. Res.* **2003**, 36, 659-667
- [70] G. Arrayas, R. Adrio, J. Carretero, *Angew. Chem. Int. Ed.* **2006**, 45, 7674-7715.
- [71] S. Toma, J. Csizmadiova, M. Meciarova, R. Sebesta, *Dalton Transactions* **2014**, 43(44), 16557-16579
- [72] N. Butt, D. Liu, W. Zhang, *Synlett* **2014**, 25(5), 615-630
- [73] M. Drusan, R. Sebesta, *Tetrahedron* **2014**, 70(4), 759-786.
- [74] D. Schaarschmidt, A. Hildebrandt, S. Bock, H. Lang, *J. Organomet. Chem.* **2014**, 751,742-753
- [75] D. Schaarschmidt, M. Grumbt, A. Hildebrandt, H. Lang, *Eur. J. Org. Chem.* **2014**, 6676–6685.
- [76] P. Štěpnička, I. Císařová, *Inorg. Chem.* **2006**, 45, 8785–8798.
- [77] P. Štěpnička, M. Lamac, I. Císařová, *J. Organomet.Chem.* **2008**, 693, 446–456.
- [78] Zhu, Jun-Chao; Cui, Dong-Xiao; Li, Yue-Dan; Jiang, Ru; Chen, Wei-Ping; Wang, Ping-An *ChemCatChem* **2018**, 10(5), 907-919
- [79] J. Podlaha, P. Štěpnička, J. Ludvík, I. Císařová, *Organometallics* **1996**, 15, 543–550
- [80] F. Barrière, R. U. Kirss, W. E. Geiger, *Organometallics* **2005**, 24, 48–52.
- [81] B. D. Swartz, C. Nataro, *Organometallics* **2005**, 24, 2447–2451.
- [82] M. Korb, D. Schaarschmidt, M. Grumbt, M. König, H. Lang, *Eur. J. Inorg. Chem.* **2020**, *accepted*.
- [83] S. Bayda, A. Cassen, J.-C. Daran, C. Audin, R. Poli, E. Manoury, E. Daydier, *J. Organomet. Chem.* **2014**, 772–773, 258–264;
- [84] M. Korb, J. Mahrholdt, H. Lang, *Eur. J. Inorg. Chem.* **2017**, 4028–4048
- [85] M. Korb, J. Mahrholdt, X. Liu, H. Lang, *Eur. J. Inorg. Chem.* **2019**, 973–987.
- [86] M. J. Verschoor-Kirss, O. Hendricks, C. M. Verschoor, R. Conry, R. U. Kirss, *Inorg. Chim. Acta* **2016**, 450, 30–38.
- [87] M. A. Bennett, S. K. Bhargava, A. M. Bond, I. M. Burgar, Si-Xuan Guo, G. Kar, Steven H. Privér, J. Wagler, A. C. Willis, A. A. J. Torriero, *Dalton Trans.* **2010**, 39, 9079–9090.
- [88] C. Hansch, A. Leo, R.W. Taft, *Chem. Rev.* 91, 165-195.
- [89] A.A. Isse, L. Falcicola, P.R. Mussini, A. Gennaro, *Chem. Comm.* **2006**, 344-346.
- [90] A.A. Isse, P.R. Mussini, A. Gennaro, *J. Phys. Chem. C* **2009**, 113, 14983-1499

WILEY-VCH

Accepted Manuscript